

# INDUCING BIOACTIVITY IN DENTAL PORCELAIN THROUGH BIOGLASS®

## Changes in thermal behaviour\*

X. Chatzistavrou<sup>1</sup>, K. Chrissafis<sup>1</sup>, E. Polychroniadis<sup>1</sup>, E. Kontonasaki<sup>2</sup>, P. Koidis<sup>2</sup> and K. M. Paraskevopoulos<sup>1\*\*</sup>

<sup>1</sup>Solid State Physics Section, Physics Department, Aristotle University of Thessaloniki, 54124 Thessaloniki, Greece

<sup>2</sup>School of Dentistry, Department of Fixed Prosthesis and Implant Prosthodontics, Aristotle University of Thessaloniki 54124 Thessaloniki, Greece

Dental materials restore morphology and function of lost or destroyed teeth, but cannot completely rebuild the structural relationship with soft periodontal tissues. The induction of bioactivity on classic dental porcelain can be achieved through the addition of bioactive glass. The aim of this study was to investigate the effect of Bioglass® on the thermal properties of dental porcelain in order to correlate the proportions of mixtures with the changes in thermal properties. Differential thermal analysis was performed in order to determine the characteristic temperatures of the mixtures. The increase of bioactive glass concentration in mixtures induces a shift to lower temperatures of the melting point temperature. This observation is attributed to the substitution of silicon ions by aluminium ions and to the formation of Al–O bond, which is weaker than Si–O bond. Mixtures heated at 950°C were examined also by the transmission electron microscopy (TEM) in order to be studied the microstructure of these samples at this critical temperature. The observed microstructural changes, confirm the process of substitution of Si<sup>4+</sup> ions by Al<sup>3+</sup> ions.

**Keywords:** Bioglass®, dental porcelain, DTA, TEM, thermal properties

## Introduction

Porcelain holds a special place in dentistry because, notwithstanding the many advances made in composites and glass-ionomers, it still is considered to produce the most pleasing result. Dental porcelain is chemically very stable and provides excellent aesthetics that do not deteriorate with time. The thermal conductivity and the coefficient of thermal expansion are similar to those of enamel and dentine, so in the presence of a good marginal seal, marginal percolation is less likely to be a problem [1].

Bioactive materials are extensively applied in areas of restoration such as orthopedic and dentistry and for this reason their study presents great interest. These materials can stimulate a specific response in the surrounding tissues by means of a complex mechanism involving three main phases: ion leaching, partial dissolution of the glass surface and precipitation of bone like apatite layer on the glass surface. Thanks to the precipitated apatite layer, these materials can provide a very strong chemical bond with both hard and soft tissues. These materials have been proposed both in bulky and in coating form for several kinds of applications. Among other materials that are used in the repair and reconstruction of diseased or damaged hard tissues (bones and teeth),

bioactive glass attracts special interest [2, 3]. Bioactive glass that show a peculiar reactivity when put in contact with human body fluids fulfills the standards for restorative dental applications, like compatibility with the oral environment. Moreover, its surface properties, such as shade translucency, toughness and wear correspond to those of natural teeth [4].

Fixed ceramic restorations restore the morphology and function of lost or destroyed teeth, but cannot completely rebuild the structural relationship with soft periodontal tissues, while a bioactive glass elicits a bioactive behavior on gingival cells of soft periodontal tissues around the margins of conventional fixed ceramic restorations. Thus, the fabrication of coating from dental porcelain with bioactive glass on dental ceramics used in metal-ceramic restorations, could provide a bioactive surface which in combination with a tissue regenerative technique could lead to periodontal tissues attachment. Surface treatment of dental ceramics with bioactive glass has already been reported [5]. As it can be understood, the examination of these materials and specially the thermal analysis of mixtures of dental ceramics with bioactive glass, presents special interest since these mixtures are used in many dental applications after a thermal treatment, which causes the change of many properties of these materials [6].

\* Presented at MEDICTA Conference 2005, Thessaloniki, peer reviewed paper.

\*\* Author for correspondence: kpar@auth.gr

The examination of the effects of the Bioglass<sup>®</sup> insertion on the thermal behaviour of porcelain was the aim of this study. In particular we studied, under the same conditions, the thermal behavior of pure porcelain and Bioglass<sup>®</sup>, as well as mixtures of porcelain and Bioglass<sup>®</sup> in three different mass ratios. The thermal parameters of the samples have been measured with differential thermal analysis (DTA). Additionally, the DTA results were correlated with the findings from the investigation of microstructural changes of these mixtures. This study was performed by transmission electron microscopy (TEM) at the critical temperature of 950°C, since the heat treatment of these composite materials is taking place at this temperature in many applications.

## Experimental

### Materials and methods

Porcelain (IPS Classic Margin, Ivoclar, Schaan, Liechtenstein) contains 55–60% SiO<sub>2</sub>, 12–15% Al<sub>2</sub>O<sub>3</sub> and 6–15% oxides of K, Na, Ca, Li in mass%, while Bioactive glass powder PerioGlas<sup>®</sup> (Bioglass<sup>®</sup> Synthetic Bone Graft Particulate, US Biomaterials) contains 45% SiO<sub>2</sub>, 24.5% Na<sub>2</sub>O, 24.5% CaO and 6% P<sub>2</sub>O<sub>5</sub>. Bioglass<sup>®</sup> with particle size range of 90–710 μm was ground in an agate mortar and it was sieved in order to obtain a powder with a particle size range 20–63 μm. Porcelain powder was then mixed with bioactive glass powder in three different proportions: 90–10 (PB10), 67–33 (PB33) and 50–50 (PB50) in mass%, respectively.

Thermal analysis was performed with a Setaram Thermogravimetric-Differential Thermal Analyzer SETSYS 1750-TG-DTA 1750°C rod. The heating rate was 10°C min<sup>-1</sup> up to a maximum temperature of 1400°C, in argon atmosphere, on each sample were determined the three main thermal parameters, the glass transition ( $T_g$ ), the crystallization temperature ( $T_c$ ) and the melting ( $T_m$ ) temperature. The thermal analysis of samples was performed up to 1400°C, since it is known that the characteristic processes of these materials (glass transition, crystallization and melting) take place at temperatures lower than 1400°C [7–9]. The TEM study was performed with a conventional TEM working on 100 kV (JEM 100C). Appropriate specimens were prepared by mechanical polishing and ion beam thinning.

## Results and discussion

The DTA curve of pure porcelain (Fig. 1e) does not present any glass transition and crystallization pro-

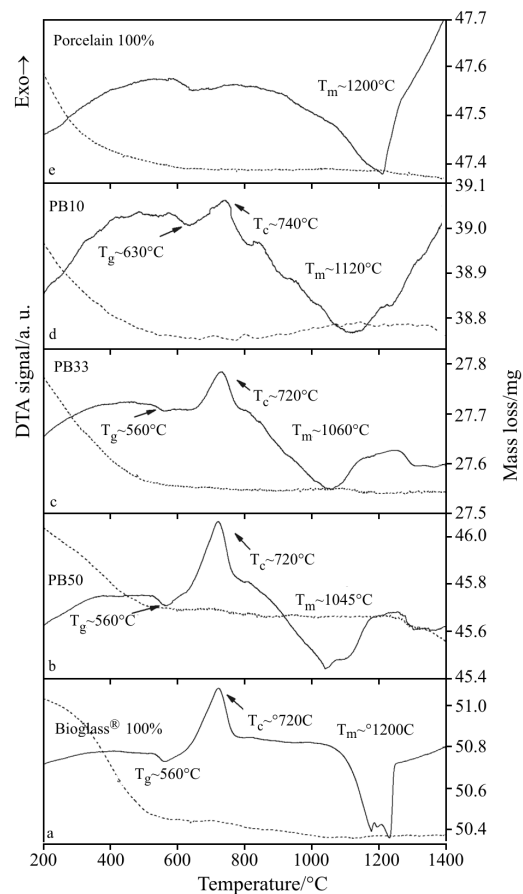


**Fig. 1** TG and DTA curves of pure porcelain and Bioglass<sup>®</sup> and their mixtures

cesses and there is only a melting process which occurs at 1200°C. The small endothermic process, at ~625°C that is detectable in the DTA curve of pure porcelain and PB10 is attributed to a crystallographic transformation of Leucite (KAlSi<sub>2</sub>O<sub>6</sub>) crystals – which are used as a reinforcing phase in some compositions for all ceramic dental restorations – from tetragonal to cubic [9]. This process is not important and becomes less observable in the thermal curves of heat treated mixtures with less participation of porcelain. At sample PB10 the participation of porcelain is significant and the transformation process of leucite crystals is observable. On the other hand, from the thermal curve of Bioglass<sup>®</sup>, can be determined the glass transition ( $T_g$ ), the crystallization ( $T_c$ ) and the melting ( $T_m$ ) temperatures. Particularly, Bioglass<sup>®</sup> (Fig. 1a) presents an endothermic peak at 560°C caused by the glass transition, followed by an exothermic event at 720°C related to the formation of crystals phases and a melting process is observed in the range 1100–1250°C. Moreover, for pure Bioglass<sup>®</sup>, it has been found that its chemistry does not vary with heating from 800 to 1000°C. Regarding the complex structure of the DTA curve at 1200°C, in our previous work on bioactive glass behavior beyond melting temperature, it was noticed that

at 1200°C take place successive crystallizations and fusions of new phases as Pseudo-Wollastonite (PsW,  $\alpha$ -CaSiO<sub>3</sub>) and Wollastonite (W,  $\beta$ -CaSiO<sub>3</sub>) with PsW being the major phase in this temperature range (Fig. 1a) [10].

The DTA curves of the mixed samples PB33 and PB50 (Figs 1b and c), show a similar thermal response as that of Bioglass<sup>®</sup> until 800°C – where the crystallization process has been completed – there is an endothermic peak at 560°C caused by the glass transition and an exothermic peak at 720°C caused by the crystallization of similar phases. A similar thermal behavior is presented by the PB10 samples, although, the transformation of leucite crystals from tetragonal to cubic causes a small delay of the glass transition and crystallization processes at higher temperatures. However, the processes of glass transition and crystallization, of the specific phases, are still observed and become more noticeable by subtracting this part of transformation from the specific curve. This behavior is attributed to the significant effect that porcelain has on the thermal behavior of the specific kind of mixed sample, since porcelain participates in that mixture with high percentage. On the other side, all mixtures present different thermal behavior in temperatures above 800°C. Consequently, it can be considered that in temperatures under 800°C – in the temperature range where the glass transition ( $T_g$ ) and crystallization temperatures are found –, all mixed samples present almost the same thermal behavior.

It should be mentioned that in Figs 1a–e the dotted line presents the mass loss e.g. how the mass of the samples changes during the thermal treatment. As it is clear, at lower temperatures there is a small reduction in the samples' mass approximately equal to 0.4% for pure porcelain, 0.4% for PB10, 0.8% for PB33, 0.9% for PB50 and 1.3% for pure Bioglass<sup>®</sup>, which is attributed to the evaporation of water that is included in samples, while at higher temperatures there is no further reduction of samples' mass. Therefore the changes of samples' mass are very small and the smaller changes which are observed at TG curves of certain samples, are out of interest. Finally, in Fig. 2 are presented the DTA curves of all mixtures and of pure porcelain and pure Bioglass<sup>®</sup>, in the melting process region: It is easily followed the shift of the melting temperature to lower values in mixtures, with the increase of the content of Bioglass<sup>®</sup>.

In details, the melting process minimum temperature of the pure porcelain is at 1200°C, while the addition of bioactive glass to the porcelain in 10%, reduces this temperature to 1120°C (Fig. 1d). Moreover, the increase of Bioglass<sup>®</sup> concentration to 33% shifts the melting point to 1060°C (Fig. 1c) and finally the increase of bioactive glass at 50%, causes a further re-

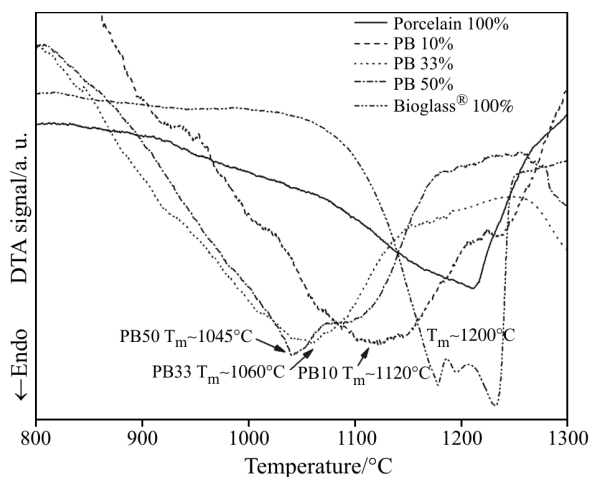


Fig. 2 The shift of melting point temperature

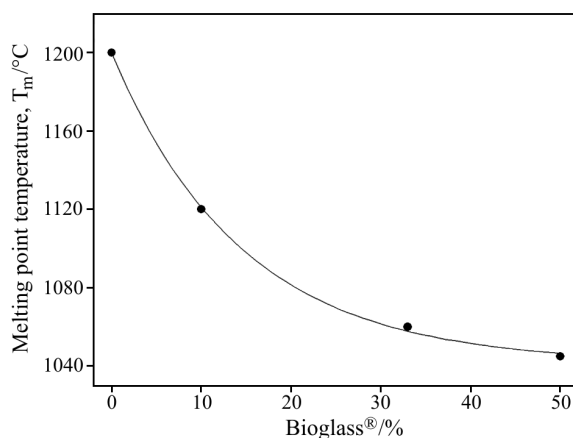


Fig. 3 Porcelain melting temperature vs. Bioglass<sup>®</sup> %.  
The solid line is guide to the eye

duction of the melting point temperature at 1045°C (Fig. 1b). The above results are summarized in Fig. 3, where the behavior of melting process temperature with the addition of Bioglass<sup>®</sup> is presented.

The shift of the melting point temperature with the addition of bioactive glass can be attributed to the formation of AlO bond, which is weaker than SiO bond. In details, the ion Al<sup>3+</sup> has an ionic radius very similar to that of the Si<sup>4+</sup> ion and therefore, it can replace the silicon ion and take part in the structure of the silicate network. However, the replacement of silicon by aluminium ions is associated with a reduction of the number of bridging oxygen ions, since aluminium atoms are in part six-fold coordinated, AlO<sub>6/2</sub><sup>3-</sup> units, and aluminium acts as network modifier producing non-bridging oxygen atoms [11–13]. This behavior weakens the silicate network by breaking its continuity and leads to a decrease in the viscosity of the glass and to a decrease in the melting point temperature ( $T_m$ ) [14].

Generally, the function of network-modifying oxides is to partly disrupt this network structure, through

the introduction of ionic bonds, so that the fusion temperature is reduced. This is achieved via the cations, which are accommodated outside of the network. These cations are not necessarily static in the structure and may migrate from one ligand environment to another. However, excessive modification via network-modifying oxides can increase the chemical reactivity of the glass, with increased tendencies towards dissolution and devitrification [15].

It is observed that at temperatures under 800°C no important changes, due to the addition of Bioglass® are appeared, as the dissolution of alumina takes place at higher temperatures, above this temperature range. Consequently, there is no release of aluminium ions, which replace silicon ions and cause the ‘interaction’ of Bioglass with the porcelain, since the dissolution of alumina starts at 900°C [16].

The role played by a cation in a glass may be classified as network former, intermediate and modifier by simple general criteria based upon bond energies and ionic field strengths [11]. The incorporation of foreign cations – of valence lower than 4<sup>+</sup> – is considered to accelerate the transition, as it provides a charge compensation mechanism – by the formation of oxygen vacancies – that enhance the transport of atoms and accelerate a phase transition [17].

Dietzel [12, 18] ordered cations according to their field strength. The field strength is defined as  $z/r^2$  where  $z$  is the valence and  $r$  the radius of ion. In particular in oxides, Dietzel examined direct Coulombic interactions between cations and anions:

$$\text{Attractive force} = \frac{(z_c e)(z_a e)}{(r_c + r_a)^2} \quad (1)$$

where  $z_c$ ,  $r_c$ ,  $z_a$  and  $r_a$  are the valence and the radius of cation and anion respectively and  $e$  the elemental charge.

For the field strength (FS) the Eq. (1) can be written:

$$\text{FS} = \frac{z_c}{a^2}, \text{ where } a=(r_c+r_a) \quad (2)$$

The cations with high field strength have high cation-oxygen bond energy. If the field strength of an oxide is  $\text{FS} > 1.3$ , it is expected to have a former character, if the field strength is  $\text{FS} < 0.4$  then it is a glass modifier and in case of the field strength being in between these values ( $0.4 < z_c/a^2 < 1.3$ ), the oxide is characterized as intermediate. Intermediate oxides do not form glasses by themselves, but act like glass formers when combined with others. Consequently alumina acts as an intermediate, because:

$$r(\text{Al}^{3+}) = 0.53, r(\text{O}^{2-}) = 1.40 \Rightarrow a = 1.93$$

$$z_c = +3 \Rightarrow z_c/a^2 = 0.8$$

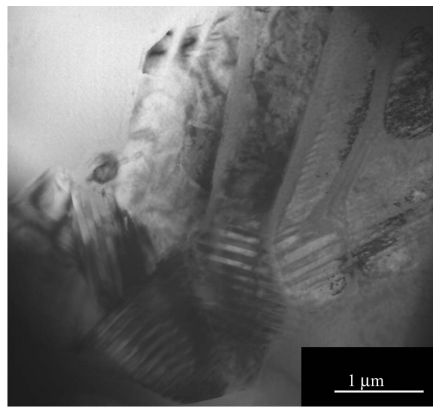


Fig. 4 TEM dark field image taken from a leucite crystal

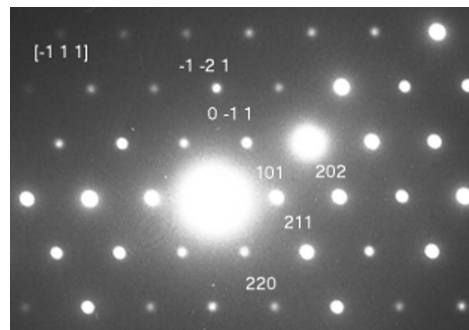


Fig. 5 Electron diffraction pattern of the leucite crystal

Although at high content, does the alumina act as modifier contributing to formation of non-bridging oxygens. The interconnected microstructure of a glass ceramic is modified and becomes relatively coarser with alumina participation above a certain value [12].

The above described behavior is confirmed by TEM results from the investigation of the microstructural changes of the mixtures, under the specific heat treatment at 950°C. Particularly, all samples present a common image of a characteristic phase. This image is a leucite (KAlSi<sub>2</sub>O<sub>6</sub>) crystal (Fig. 4), with a corresponding diffraction pattern, which is presented in Fig. 5.

Leucite crystal at room temperature is crystallized in tetragonal system and the values of the characteristic lattice parameters are presented in Table 1 [19, 20]. As it was mentioned above, it is known that leucite undergoes

Table 1 Characteristic lattice parameters of leucite crystal, tetragonal system

<i>a</i>	<i>b</i>	<i>c</i>	α/°	β/°	γ/°
12.931	12.931	13.812	90	90	90

Table 2 Characteristic lattice parameters of leucite crystal after heat treatment at 950°C, orthorhombic system

<i>a</i>	<i>b</i>	<i>c</i>	α/°	β/°	γ/°
13.432	13.049	12.916	90	90	90

a crystal transformation from tetragonal to cubic at 625°C, however in our samples, was observed a different behavior, since the values of the characteristic lattice parameters are slightly different from those that were expected. Specifically, the exact values of the lattice parameters (Table 2) confirm that due to the specific heat treatment of the samples, the initial tetragonal crystallographic system of leucite crystals has been transformed to an orthorhombic system.

This deformation is exclusively owned to the substitution of  $\text{Si}^{4+}$  ions by  $\text{Al}^{3+}$  ions, in the crystal lattice of leucite crystals. Thus, from TEM investigation is also confirmed the process of substitution, which takes place under the specific heat treatment, since leucite undergoes a crystal transformation from tetragonal to orthorhombic at 950°C.

## Conclusions

From the thermal study of mixed samples (porcelain with Bioglass<sup>®</sup>), it was observed that a) all mixed samples present parallel thermal behavior with that of pure Bioglass 45S5 until the crystallization temperature, as the dissolution of alumina starts at higher temperatures, and b) the melting process temperature shifts to lower temperatures with the increase of concentration of bioactive glass. This shift with the addition of Bioglass<sup>®</sup> is attributed to the formation of AlO bonds and alumina is thought to act as network modifier producing non-bridging oxygen atoms. The substitution of  $\text{Si}^{4+}$  ions by  $\text{Al}^{3+}$  ions was confirmed by TEM, where in SAD patterns of leucite crystals was observed a microstructural deformation of these crystals from tetragonal crystallographic system to orthorhombic system.

## Acknowledgements

It is acknowledged the support of the Greek Ministry of Education and European Community under the program Pythagoras II.

## References

- 1 R. Van Noot, An Introduction to Dental Materials, 2<sup>nd</sup> Edition, Mosby 2002.
- 2 A. S. Rizkalla, D. W. Jones, D. B. Clarke and G. C. Hall, *J. Biomed. Mater. Res.*, 32 (1996) 119.
- 3 E. Verne, C. Vitale Brovarone and D. Milanese, *J. Biomed. Mater. Res.*, 53 (2000) 408.
- 4 W. Holand, *J. Non-Cryst. Solids*, 219 (1997) 192.
- 5 E. Kontonasaki, L. Papadopoulou, T. Zorba, E. Pavlidou, K. Paraskevopoulos and P. Koidis, *J. Oral Rehab.*, 30 (2003) 1.
- 6 L. Papadopoulou, E. Kontonasaki, T. Zorba, X. Chatzistavrou, Pavlidou, K. Paraskevopoulos, S. Sklavounos and P. Koidis, *Phys. Status Solidi A*, 198 (2003) 65.
- 7 K. Tonsuaadu, M. Peld and V. Bender, *J. Therm. Anal. Cal.*, 72 (2003) 363.
- 8 S. C. Mojumdar, J. Kozankova, J. Chocholousek, J. Majling and D. Fabryova, *J. Therm. Anal. Cal.*, 78 (2004) 73.
- 9 I. L. Denry, J. A. Holloway and S. F. Rosenstiel, *J. Biomed. Mater. Res.*, 41 (1998) 398.
- 10 X. Chatzistavrou, T. Zorba, E. Kontonasaki, K. Chrissafis, P. Koidis and K. M. Paraskevopoulos, *Phys. Status Solidi A*, 201 (2004) 944.
- 11 A. Aronne, S. Esposito and P. Pernice, *Mater. Chem. Phys.*, 51 (1997) 163.
- 12 E. Demirkenes and E. Maytalmán, *Ceram. Inter.*, 27 (2001) 99.
- 13 D. U. Tulyaganov, M. J. Ribeiro and J. A. Labrincha, *Ceram. Inter.*, 28 (2002) 515.
- 14 I. L. Denry and J. A. Holloway, *J. Biomed. Mater. Res.*, 63 (2002) 146.
- 15 N. Ray, *Dental Materials Science, Ceramics in Dentistry*, 1998, Chapter 10 p. 112.
- 16 C. B. Hong and K. H. Lee, *PRICM-2: Proc. of the Second Pacific Rim Int. Conf. on Advanced Mater and Processing*, Eds K. S. Shin, J. K. Yoon and S. J. Kim, The Korean Institute of Met. Mater., Korea 1995.
- 17 K. Okada, N. Yamamoto, Y. Kameshima and A. Yasumori, *J. Am. Ceram. Soc.*, 84 (2001) 1591.
- 18 K. Franks, I. Abrahams, G. Georgiou and J. C. Knowles, *Biomater.*, 22 (2001) 497.
- 19 F. Mazzi, E. Galli and G. Gottardi, *Am. Miner.*, 61 (1976) 108.
- 20 D. C. Palmer, E. K. H. Salje and W. W. Schmahl, *Phys. Chem. Miner.*, 16 (1989) 714.

---

Received: July 3, 2005

Accepted: November 3, 2005

OnlineFirst: August 11, 2006

---

DOI: 10.1007/s10973-005-7166-x